

Path-Following Guidance Using Phantom Sensation Based Vibrotactile Cues Around the Wrist

Jose V. Salazar L., Keisuke Okabe, and Yasuhisa Hirata

Abstract—Vibrotactile feedback systems for supporting human motion have been widely researched, mainly owing to the low price and reduced size of vibration motors, which allow trainees to actively move while using them. Most existing vibrotactile feedback systems focus on providing information about the human’s joint angles, making it necessary to understand multiple simultaneous stimuli to guide the trajectory of a limb. Instead, in the present study, we focus on guiding the motion of the hand by following an endpoint approach and propose a vibrotactile feedback paradigm to convey direction around the wrist and guide the user’s wrist around points in a two-dimensional Cartesian space. In the path-following task, vibrotactile cues are provided as direction information to modify the wrist’s path only when the wrist’s position deviates significantly from the desired path. The experiment was designed based on the motor learning process to observe the evolution of performance during training. We found that the root mean squared error of participants decreased by 49.3% when provided with vibrotactile feedback. This effect was almost constant throughout training. Additionally, most participants could reproduce the desired path after removing the provided feedback immediately after training. We believe the proposed system can be applied to enhance the process of learning tasks that require hand guidance, such as learning of Japanese calligraphy or upper limb rehabilitation.

I. INTRODUCTION

In various domains such as sports and rehabilitation, it is common to receive guidance from experts or watch videos to learn a specific motor skill. Usually the trainee performs a motion, the instructor then qualitatively evaluates the movement, takes their hand, and demonstrates the correct movement or teaches the trainee through a step by step process. Recent developments in hardware and sensing technologies have enabled researchers to provide motion guidance by using robotic technologies in a manner similar to human instructors.

A few examples include the use of PHANToM haptic device (SensAble Technologies, Inc.), which provides force feedback for rehabilitation of the upper limbs [1] or surgical training [2]. Exoskeleton-type systems that calculate the target angle of each joint using the target arm motion and guide the user’s joint angles have also been proposed [3] [4]. Granados et al. [5] developed a dance-teacher-type robot that physically interacts with trainees and takes the leading role in ballroom dancing. This robot evaluates the user’s performance based on practice history and tailors feedback

accordingly.

To facilitate safe human-robot interaction, haptic guidance systems based on the concept of passive robotics [6] (i.e., the system that does not have a driving force) have been proposed as well. Koyanagi et al. [7] developed an arm-type haptic guidance system that uses electrorheological (ER) fluid brakes to correct a user’s motion. Schneider et al. [8] developed a surgery support system called passive arm with dynamic constraints (PADyC) that constrains the motions of a tool along a preplanned path. Other systems that redirect the motive force applied by the user along a target direction using brakes or clutches have been developed as well [9] [10]. Furthermore, Hirata et al. [11] created a wire driven motion support system that corrects a user’s motion by generating brake tension on wires attached to a tool by using servo brakes and applied it to swing training in tennis.

In all these systems, motion guidance is achieved by limiting the motion of a human by using servo motors, brakes, and other components. In recent years, haptic devices that provide tactile cues (e.g. vibration, tapping, pressure, and skin deformation) have been proposed to improve performance in an unobtrusive way [12]. Among such devices, systems that use vibrotactile stimuli are especially popular owing to their comparatively low cost, small size of vibrotactile actuators, and the fact that they can be attached anywhere on the surface of the body. Such systems have already been applied to various motor activities such as playing musical instruments, sports, rehabilitation, and surgical training [13]–[17]. To provide richer and more intuitive cues, feedback paradigms using vibrotactile illusions have been studied as well [18]–[21].

Most of the proposed vibrotactile feedback strategies coordinate human motion from the joint angle perspective (i.e., correcting each joint’s angle with localized vibrotactile cues) [13]–[21]. However, understanding multiple simultaneous cues becomes more difficult as the number of cues increases [22] [23]. Additionally, in tasks such as learning Japanese calligraphy, component assembly, dance, and rehabilitation, the motion depends mainly on the hand position, which is why an endpoint or end-effector-based feedback strategy is desirable.

As an example of an end-effector guidance strategy, we can mention the work of Basu et al. [16], in which users were trained for a needle insertion task by applying vibrotactile feedback on the forearm to provide guidance for joint, cartesian, and tool spaces, with the latter proving to be the most effective approach. Despite this study, end-effector approaches remain uncommon, which might be due to the

*This work was not supported by any organization

J. V. Salazar L., K. Okabe, and Y. Hirata are with the Department of Robotics, Tohoku University, Sendai, Miyagi 980-8579, Japan [j.salazar](mailto:j.salazar@rd.mech.tohoku.ac.jp), [k.okabe](mailto:k.okabe@rd.mech.tohoku.ac.jp), hirata@rd.mech.tohoku.ac.jp

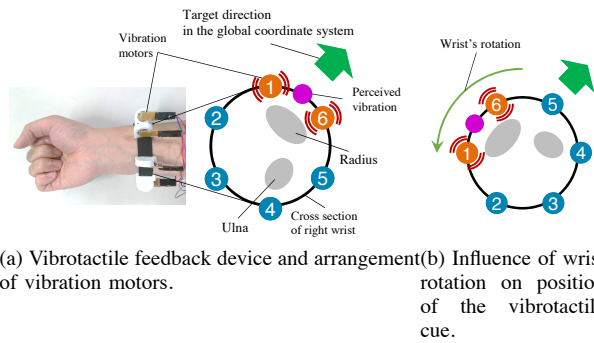


Fig. 1: Vibration motor mappings on wrist, and wrist rotation effect.

difficulty of conveying multiple directions at the end-effector.

To this end, a method has been proposed to produce a vibrotactile cue in any place around the wrist by using a wristband embedded with six vibration motors and a vibrotactile illusion called phantom sensation [24]. The generated cue is perceived as a single point vibrotactile stimulation by the user, and it can be mapped along the direction in which the wrist should be moved under two conceptual mappings, "push" and "pull." Under push mapping, users are instructed to move in the direction opposite to the stimulus location. Conversely, under the pull mapping, they are instructed to move toward the direction in which they felt the cue. Users were able to localize the cue around the wrist with an error of around 10° and were able to follow the cues and move their wrist to specific target positions in a two-dimensional plane under both conceptual mappings. When moving the wrist, users adjust the angles of the arm's joints accordingly by using a single cue.

In the present study, we use a variation of this paradigm to guide users while moving their wrist through a predetermined path. Instead of conveying direction continuously, vibrotactile cues are only produced when the wrist deviates from a deadband around the path, thus correcting the motion. In this manner, feedback is less intrusive, which allows the user to focus more on the motion and proprioceptive information. Experimental results show that the position error during training is significantly reduced by using the cues and most users can reproduce the path more accurately after training.

The remainder of this paper is organized as follows: In section II, we present an overview of the method to convey direction, which was introduced in our previous work, and the system configuration. In section III, we explain the vibrotactile feedback approach to achieve path-following guidance. In section IV, we present the experimental framework and results. Finally, section V presents our conclusions.

II. HAPTIC GUIDANCE SYSTEM FOR THE WRIST

A. Wrist Guidance Paradigm

In our previous research, we proposed an approach to convey direction by providing only one vibration stimulus at a certain location on a user's wrist [24]. In this method, we used phantom sensation, which is an illusion that causes

users to feel an averaged vibration when two vibrotactile cues at a close distance are applied to the skin. The perceived location of the virtual cue varies depending on the relative amplitude of the two actual cues. By arranging equally spaced vibration motors around the wrist, we can generate a vibrotactile cue at any location around the wrist, including those parts where no vibration motor is present. In our paradigm, when the direction to be displayed coincides with the physical location of a motor, we use that motor to generate the cue; else, we select the two surrounding vibration motors and calculate the actuation driving voltage of each motor according to the direction in which we want to provide the cue.

The advantage of this algorithm is that the location at which the vibration is produced can be changed instantaneously, thus changing the displayed direction. In addition, we can define conceptual mappings that suit the corresponding task (e.g., moving the wrist toward the direction in which the vibration is felt and in the opposite direction).

In this approach, even if we cause the motors to actuate based on the target direction in the local coordinate system (the arrangement of motors is shown in the Fig. 1a), the motors are rotated along with the wrist. Consequently, the vibrotactile cue is perceived by the user in a direction different from the target direction, as can be seen in Fig. 1b. Therefore, we need to compensate for wrist rotation when determining which motors to actuate in the local coordinate system. To this end, we calculate the direction of the vibrotactile cue as the difference between the target direction in the global coordinate system and the wrist angle, which is measured using an inertial measurement unit (IMU), in the local coordinate system. Then, we determined which motors should be actuated to generate a cue at this location. Consequently, the user can perceive a vibrotactile cue consistent with the global coordinate system, independent of wrist rotation.

B. System Configuration

The developed haptic device is shown on the left side in Fig. 1a. In this device, six modules embedded with vibration motors are attached to a rubber band. The modules are made of acrylonitrile-butadiene-styrene, which is rigid and effectively conveys motor vibration to the skin. We used pancake-type eccentric vibration motors (FM34F) manufactured by TOKYO PARTS Corp. The modules were placed against the skin so that the direction in which the vibration was stronger (parallel to the base of the motor) was perpendicular to the skin. Additionally, a smaller contact surface with the skin was thought to be closer to the ideal condition of a point-type vibration, instead of conveying vibration over a large area of the skin. The number of actuators was set to six based on the average circumference of the wrist (≈ 16.5 - 19.0 cm among men over 165 cm tall [25]) and the ideal distance to produce the phantom sensation (between 4 and 5 cm [26]). When using the device, we can manually adjust the six actuator modules such that they are spaced evenly around the wrist. The voltage of each actuator was controlled using 12-bit pulse width modulation (PWM) within the rated

voltage range (2.5 V to 3.5 V) of the motor. To measure the wrist angle, we used an IMU (LSM9DS0) from Adafruit filtered using a Madgwick filter. The system was controlled using a Raspberry Pi Zero W that communicates with PCs via Wi-Fi.

III. MOTION ASSISTANCE APPROACH

A. Control Strategy

In the paradigm to convey direction, as proposed in our previous study, the vibrotactile cue is generated steadily, and its position can be changed instantaneously [24]. Using this paradigm, a direction can be specified continuously to guide users while following a path.

However, such sustained vibrotactile cues throughout the task are rather disruptive stimuli, which can result in mental fatigue, reduced skin sensitivity, irritation, or loss of concentration [27] [28]. Furthermore, providing such frequent feedback can result in overcorrection of the motion, and users can become dependent on feedback. The task then changes to following the feedback, instead of focusing on the motion. It has been reported that performance is lowered significantly by such feedback [29] [30].

These problems can be avoided by providing feedback only when the movement is outside of a predetermined error tolerance [29]. Indeed, multiple motion guidance approaches based on the abovementioned concept have been proposed. Stanley et al. applied this concept to guide wrist rotation by using different approaches and set a region called as "deadband", in which feedback is not provided [12]. Similarly, Bark et al. defined an area around the desired joint angles of the wrist, upper arm, and elbow as deadband, where no vibrotactile feedback is provided [22].

In the present study, we use the concept of deadband for a wrist guidance task that employs vibrotactile cues. When the wrist deviates from the deadband, a vibrotactile cue is generated to restore the user's wrist position to the desired path. The cue is mapped to the direction under the "push" mapping, which is similar to Lieberman's approach of producing a vibrotactile cue in the direction opposite to which the user should move for correcting joint angles [18]. In our previous study [24], a few participants declared that it felt natural to move away from the vibration, and it was easier than precisely localizing its source, so we decided to instruct users to follow a "push" conceptual mapping. In addition, we thought this mapping would be very intuitive because the user would feel the vibration as a disturbance and then be compelled to escape from it.

To calculate the direction of cues so that any deviation from that desired path would cause a restoring vibration to move the wrist towards the desired path, we generated a vector field around the desired path.

B. Vector Field Generation

In path-following control of mobile robots or manipulators, a few techniques employ vector fields, such as Khatib's artificial potential method [31] and Dellon's path-following vector generation [10]. The artificial potential method is

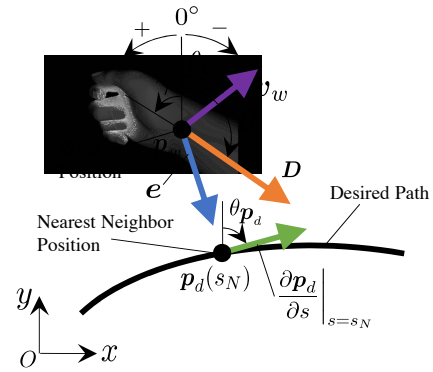


Fig. 2: Method of vector field generation.

often used when a mobile robot performs path planning while avoiding obstacles online. Contrastingly, the path-following vector generation method is used when calculating parameters such as speed are based on the relative error between the mobile body and a reference point on the path, if the path is known.

We believe the path-following vector generation concept can be applied to determine the direction and amplitude of the vibrotactile cues to guide the user when the wrist moves away from the deadband.

We define the desired path as a parametric curve represented by $\mathcal{P} = p_d(s) \in \mathbb{R}^2$. The value $s \in [s_{start}, s_{goal}]$ is a parametric variable. To guide the wrist position along the desired path, the user should move the wrist toward direction D , which combines the direction to correct the deviation and the direction leading to the end point of the path, as shown in Fig. 2. Hence, D can be calculated as follows:

$$D = K_p \left. \frac{\partial p_d}{\partial s} \right|_{s=s_N} + K_o e, \quad (1)$$

where s_N is a parameter indicating the point on the desired path that is nearest to the wrist position p_w , K_p , K_o are two diagonal matrices of 2×2 with gain elements, and e is the deviation between p_w and the nearest neighbor point on the desired path $p_d(s_N)$. We can calculate the direction of vector D obtained from Eq. (1) with respect to the global coordinate system as follows:

$$\theta = \begin{cases} \frac{\pi}{2} + \arctan \frac{D_y}{D_x} & \text{if } D_x < 0 \\ \frac{\pi}{2} - \arctan \frac{D_y}{D_x} & \text{if } D_x > 0 \\ \frac{\pi}{2} - \text{sgn} D_y \cdot \frac{\pi}{2} & \text{otherwise,} \end{cases} \quad (2a) \quad (2b) \quad (2c)$$

where (D_x, D_y) are the components of vector D .

As mentioned before, users follow a "push" mapping, hence the direction of the vibrotactile cue γ can be calculated as $\gamma = \theta + \pi$, which is the direction opposite to that of the desired motion. The magnitude of the vibrotactile cue A_v can be calculated as the Euclidean norm of the vector D . This value is mapped to the voltage applied to the vibration

motors, which is proportional to the amplitude of vibration. The minimum and maximum magnitudes of A_v are set to the lower and upper values of the rated voltage of the actuators. We set the minimum magnitude of the actuator as the minimum drive voltage for which users could detect vibration.

$$A_v = \begin{cases} \|\mathbf{D}\| & \text{if } \|e\| > r_{\text{deadband}} \\ 0 & \text{if } \|e\| \leq r_{\text{deadband}}, \end{cases} \quad (3a)$$

$$(3b)$$

where r_{deadband} is the width of the deadband.

Using Eq. (1), a vector field indicating the appropriate motion direction according to the wrist position can be generated. However, this method of generation has several limitations. One is a duplicate of nearest neighbor points between the desired path and the \mathbf{p}_w . The nearest neighbor point is the point on the path with the shortest distance to the wrist position. However, in a few cases, the nearest neighbor cannot be determined uniquely (e.g., near a parabolic curve). To overcome this limitation, we select the appropriate nearest neighbor point by comparing the tangential vector on the candidate with the velocity vector of the wrist. First, we calculate the Euclidean distances between the wrist position and the candidate and sort the values in descending order. Next, we calculate the difference between the tangential direction toward the endpoint of the path $\theta_{\mathbf{p}_d}$ and the direction of the wrist velocity vector θ_w , and then we add this difference to the Euclidean distance to obtain an evaluation value calculated as follows:

$$E = \|e\| + e_d, \quad (4)$$

where $e_d = |\theta_{\mathbf{p}_d} - \theta_w|$. The candidate point on the path with the smallest evaluation value E is selected as the nearest neighbor point.

Another obstacle is the time required to determine the nearest neighbor point on the path every time the wrist position is updated. To address this issue, we used a method proposed by Dellon et al. [10], in which the curve is partitioned into points and stored in a k-dimensional tree and the candidates are searched using the k-nearest-neighbors algorithm, which reduces the computational complexity to $O(\log n)$ instead of $O(n)$ in the case of a brute force search.

IV. EXPERIMENTS

A. Experimental Setup

The purpose of the experiment is to verify whether users can improve their performance in a given motor skill by using the feedback approach described in the previous section. The experiment was carried out in a space of approximately 3 m \times 3 m without obstacles, and the position of the participant's wrist was measured using a motion capture system (from Motion Analysis). The haptic device was attached to the participant's right arm. The experimental environment is shown in Fig. 3. In Fig. 3, the x - y plane corresponds to the coronal plane.

We set the size of the desired path such that participants with a height of around 170 cm could follow the path on the

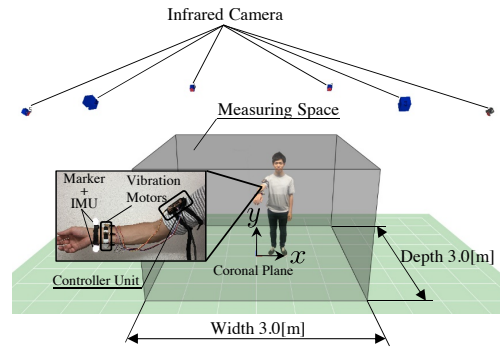


Fig. 3: Experimental environment.

plane with their wrist while bending their elbows naturally. The gain used in Eq. (2) to generate the vector field was set to $\mathbf{K}_p = \text{diag}(600.0, 600.0)$, $\mathbf{K}_o = \text{diag}(8.0, 8.0)$. We selected this value so that the magnitude of the vectors along the borders of the deadband exceeded the minimum magnitude of vibration that can be felt by the users. The resulting vector field is shown in Fig. 4.

B. Experimental Protocol

The experiment comprised four phases. At the beginning of each phase, participants were guided toward the start point by using a continuous vibrotactile cue, as proposed in our previous research [24]. Then, they were requested to hold the position for 3 s, after which all motors were made to vibrate simultaneously twice to mark the start of the task. After the signal, the users moved their wrists along the desired path. When the wrist reached the goal point, all motors were activated in a burst, letting the users know they have reached the goal.

The phases of this experiment were designed based on the motor learning process model proposed by Fitts et al. [32]. According to this model, the process of learning motor skills is divided into three stages: 1) verbal-cognitive stage, 2) motor stage, and 3) autonomous stage. In the verbal-cognitive stage, a trainee understands the task. In this stage, the trainee obtains information such as the form of the motion and how quick the movement needs to be performed. In the motor stage, the trainee practices the task and learns how to execute it. By practicing, the trainee can gain information on how much their behavior deviates from the desired movement. Then, when the trainee moves to the autonomous stage, detailed attention to movement decreases, and information becomes less necessary. The phases were based on the following model:

1) Cognitive phase:

The goal of this phase was to allow participants to understand the positional relationship between the desired path and the hand and to get used to the environment. Participants were required to move their wrist while watching the wrist position and the desired path on a visual display. Moreover, they were instructed to leave the deadband on purpose to experience the vibrotactile

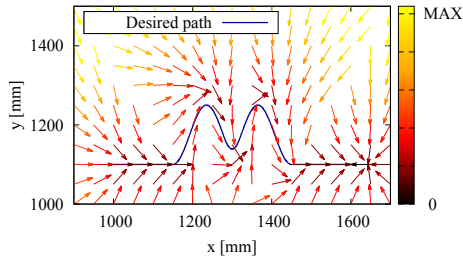


Fig. 4: Vector field of a desired path. The color represents the magnitude of each vector, which was used to calculate the amplitude of the vibrotactile cue.

feedback. The deadband was set to a radius of 30 mm around the desired path, based on the average wrist size, so the wrist can fit entirely inside the deadband. In addition, the speed of wrist movement was set to less than 200 mm/s based on humans' response time to vibration and results of preliminary experiments. If a user exceeded this wrist velocity, a beep sound was played back. In this phase, the path following task was repeated five times.

2) Preliminary test phase:

In this phase, we tested how accurately the participants were able to follow the path while trying to elicit its characteristics from the previous phase. For this test, the display was removed and the participants were asked to follow the path with no vibrotactile feedback. In this phase, the task was repeated five times.

3) Training phase:

Participants were required to repeat the motion, and vibrotactile feedback was produced when they deviated from the path. Similar to the previous phase, no display was provided. In this phase, we adjusted the deadband according to the participant's past performance, as performed by Bark et al [22]. They used the root mean squared error (RMSE) to calculate the width of the deadband. However, wrist motion inside the deadband increased the RMSE, which in turn increased the size of the deadband, even when the participant's wrist stayed within it. To overcome this limitation, we used the following evaluation metric to adjust the deadband:

$$\text{score} = O_D/T_D \quad (5)$$

where O_D is the distance calculated by summing up the Euclidean distance between consecutive data points (sampled at 200 Hz) of the traveled path while the wrist was outside the deadband throughout each trial, and T_D is the total distance the moved by the wrist. This metric was calculated for every repetition in this phase. If $\text{score} < 0.4$, we considered it a positive response. The initial width of the deadband was set to 30 mm. If a participant had three consecutive positive trials, the deadband was decreased by 2 mm. By contrast, if it was $\text{score} \geq 0.4$ even in one trial, the deadband was increased by 2 mm. The lower and upper bounds of the

deadband were set to 20 mm and 40 mm, respectively. In this phase, the task was repeated 20 times because in the preliminary experiments, we found that participants would lose focus with a greater number of repetitions.

4) Autonomous phase:

This phase is similar to the Preliminary test phase. Participants were asked to move their wrists along the desired path without vibrotactile feedback. This allowed us to measure whether the vibrotactile feedback improved or deteriorated their motor skills. In this phase, the task was repeated five times.

In the experiments conducted in the present study, participants were divided into two groups to validate the effectiveness of the proposed method. The first group, called the with feedback (WF) group followed the procedure described above. The second group, called the no feedback (NF) group, did not receive any feedback during the Training phase. Twenty male participants recruited from Tohoku University, including students and staff, participated in this experiment. Their ages ranged from 20 to 36, with a mean of 23.9 years, and their height ranged from 165 to 189, with a mean of 172.9 cm. Ten out of twenty participants had experienced vibrotactile feedback by wearing the device in previous studies. In each group, 10 participants were assigned the experiments, and the numbers of experienced and inexperienced users were balanced.

C. Results

Fig. 5, 6 show a sample of the results of the path-following task for each group. These results show the path followed by the participants in the final trial of each phase. From this graph, participant A's ability to follow the path aided with vibrotactile feedback improved in the Training and Autonomous phases compared with that in the Preliminary test phase. From Fig. 5b, the participant could correct the path by using the generated vibrotactile feedback.

Figure 7 shows the average and standard deviation of the RMSE in each phase. In the WF group, all participants could reduce the RMSE in the Training phase compared to that in the Preliminary test phase. Moreover, in the same group, six out of ten participants could reduce the RMSE in the Autonomous phase even further compared with those in the two previous phases. In the NF group, four out of ten participants could reduce the RMSE in the Training phase and Autonomous phase compared with that in the Preliminary test phase. However, their RMSE was generally higher than that of the participants in the WF group.

To test the statistical significance of the difference between the two groups, we first used Mauchly's Test to check the sphericity of all data across the three phases. As the assumption of sphericity was violated ($\chi^2(2) = 7.32, p = 0.026 < 0.05$), we conducted an ANOVA test for split-plot factorial design with Greenhouse-Geisser correction ($\epsilon = 0.74$) to evaluate followability and learning effects within each of the two groups across all phases. The results revealed a statistically significant interaction between the effects of the user's group and phase in the RMSE ($F(1.5, 26.7) = 10.0$,

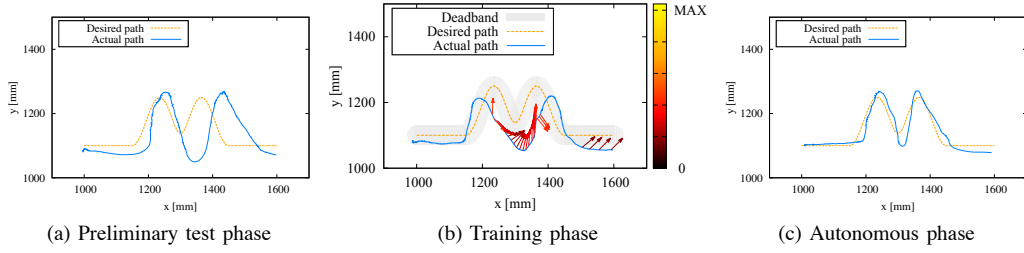


Fig. 5: Sample of the wrist positions of Participant A (WF group) in each phase. The blue line shows the path followed by the wrist. The orange dashed line shows the desired path. In (b), the filled curve indicates the deadband of the desired path with a radius of 30 mm and the vectors shows the direction suggested to the user. The color of the vector indicates the intensity of vibration.

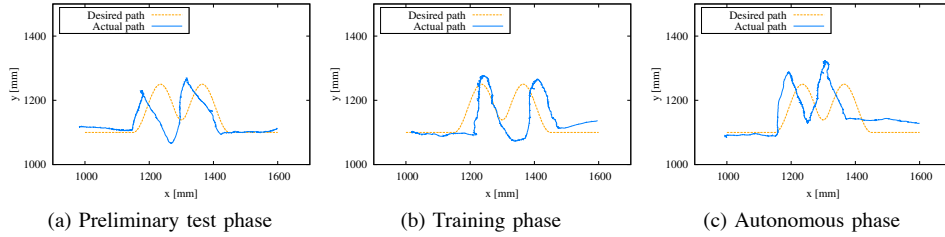
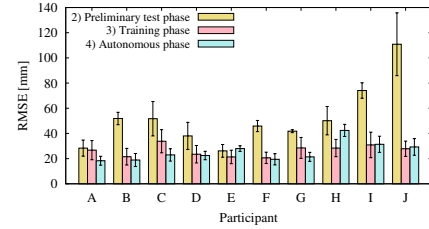


Fig. 6: Sample of the wrist position of participant K (NF group) in each phase.

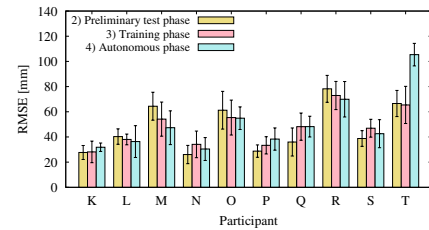
$p = 0.001$, $\eta_p^2 = 0.36$). Simple main effects analysis showed in the case when vibrotactile feedback was used, the reduction in RMSE was greater than in the case when the vibrotactile feedback was not used, as can be seen in the Training phase ($F(1, 18) = 19.6$, $p < 0.001$, $\eta_p^2 = 0.52$) and the Autonomous phase ($F(1, 18) = 11.1$, $p = 0.004$, $\eta_p^2 = 0.38$), depicted in Fig. 8. Furthermore, the RMSE of the participants in the WF group decreased for both the Training and the Autonomous phases compared with that in the Preliminary test Phase ($F(1.2, 10.3) = 11.7$, $p = 0.005$, $\eta_p^2 = 0.57$). A multiple comparison using Shaffer's modified sequentially rejective Bonferroni method within three phases revealed a statistically significant difference between the Preliminary test phase vs. the Training phase with ($t(9) = 3.57$, $p = 0.006$) and the Preliminary test phase vs. the Autonomous phase ($t(9) = 3.44$, $p = 0.007$) in case of the WF group.

Fig. 10 shows the RMSE of each participant for every task in the Training phase. We found that the RMSE tends to be lower in case of the WF group, and our statistical analysis revealed a significant difference with the results of the NF Group. From this result, we confirmed that the participants in the WF group could recognize the suggested direction based on the vibrotactile feedback and corrected the path of their wrist accordingly.

Furthermore, we observed that the RMSE did not seem to decrease further over trials in the Training phase. To test this, we performed a Friedman test for various numbers of trials in both groups, and the results of this test indicated no statistical significance (WF group: $\chi^2(9) = 9.86$, $p = 0.36$, NF group: $\chi^2(9) = 7.37$, $p = 0.60$), which confirmed our



(a) WF group (participants A, to J)



(b) NF group (participants K, to T)

Fig. 7: Average RMSE in each phase. Error bars show standard deviation.

observations.

In addition, Fig. 9 shows the changes in the width of the deadband throughout the Training phase for each participant in the WF group. Four out of ten participants (B, D, E, and F) performed very well, reaching the lower limit of the deadband width (20 mm). The mean of their RMSEs (21.7 ± 1.23) in the Training phase was smaller than the average RMSE of the remaining participants in the WF group (29.3 ± 2.57). Other participants, such as H and I, performed worse and the width of their deadband increased

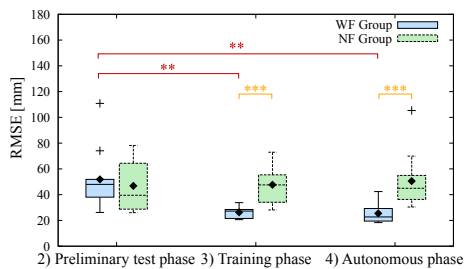


Fig. 8: Boxplot of RMSEs of all participants by group. The boxes represent the interquartile range (IQR), which contains 25% to 75% of the data. The central horizontal line inside the boxes is the median. The outliers and the mean of the data are plotted as cross marks and a spade mark, respectively. The orange and red stars represent the statistically significant differences determined by simple main effects analysis and multiple comparisons, respectively, where $**$ represents $p < 0.01$ and $***$ represents $p < 0.001$.

gradually; however, the feedback allowed them to maintain a comparatively low RMSE, especially when compared with the participants in the NF group.

D. Discussion

From the experimental results, we found that all participants in the WF group were able to correct the path of their wrist by interpreting the provided vibrotactile cues. By providing the vibrotactile feedback, the mean RMSE decreased by 49.3% between the Preliminary test phase and the Training phase, which shows that the deadband approach is effective for reducing the RMSE during training. This is in line with the results obtained by Bark et al. [22], although they combined vibrotactile feedback with visual feedback. In their research, because the motion was coordinated per joint, the error of each joint propagated and ultimately affected the position of the end-effector, and the RMSE increased for higher DoF tasks, in which the position of the end-effector deviated further. Our approach corrects the motion of the end-effector directly, which simplifies the cues while reducing the error in the end-effector position.

In the Autonomous phase, most of the participants in the WF group maintained low RMSE values, which suggests that they were able to recall the shape of motion on their own, rather than by simply following the vibrotactile cues. However, we believe it is necessary to verify the effects of the proposed approach over a long term because our experiment lasted only about 30 min. Repeating the experiments after a few days will provide insights into the effects of the proposed feedback on motor learning.

Furthermore, we observed that participants could immediately reduce their RMSE in the Training phase, but could not improve it beyond a certain threshold throughout this phase. This tendency seems to be associated with the use of the deadband approach because the motion inside the deadband cannot be further corrected. This finding suggests that changing the deadband according to the user's performance during

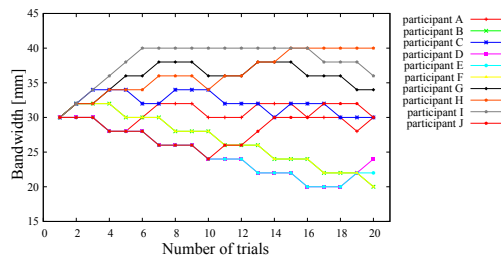


Fig. 9: Changes in deadband width in Training phase for WF group.

the Training phase has no effect. In fact, the performance of participants did not seem to be affected by changes in the deadband. Given the way in which the deadband was calculated (Eq. 5), the participants who could reduce the width of the deadband received less feedback, while those who performed worse received more feedback. Based on this fact, it is less likely that the participants who perform better become dependent on the feedback.

In addition, the speed at which participants were requested to move their wrist was around 200 mm/s. This speed was selected based on user responsiveness and the time required to locate the spot at which the vibration is produced. We believe it is necessary to evaluate how the speed of motion affects the recognition of feedback to properly design adequate approaches for activities such as sports.

V. CONCLUSION

In this paper, we proposed an approach to provide path-following guidance in the coronal plane by using phantom-sensation-based vibrotactile feedback. The location at which the vibrotactile feedback was produced on the user's wrist was calculated using a vector field generated around the desired path, and the feedback provided only when the user's wrist deviated from the specified deadband. We performed a four-phase experiment inspired by the motor learning process. We found that participants were able to follow a given path more accurately under the proposed vibrotactile feedback approach while repeating the path-following task accurately in subsequent trials without the feedback. However, further experimentation is required to determine the effects of the proposed paradigm on long term motor learning. We intend to apply the proposed paradigm for tasks that require training of hand motion (e.g., learning Japanese calligraphy, dancing, and upper limb rehabilitation).

In the future, we want to develop a feedback approach that can provide guidance for high speed motions and evaluate its effectiveness in the long term. Furthermore, we hope to extend the current approach to guidance in three-dimensional spaces to aid more complex tasks.

REFERENCES

- [1] J. B. Maniya, P. Pathak, and B. Kumar Mishra, "Design and development of virtual objects to be used with haptic device for motor rehabilitation," *Journal of Software Engineering and Applications*, vol. 3, pp. 990-997, 01 2010.

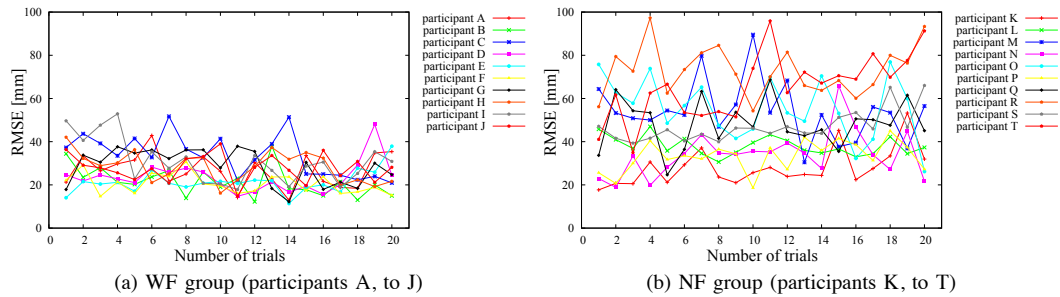


Fig. 10: Plot of RMSE for all trials in the Training phase.

- [2] M. Nambi, P. S. Bernstein, and J. J. Abbott, "Effect of haptic-interface virtual kinematics on the performance and preference of novice users in telemanipulated retinal surgery," *IEEE Robotics and Automation Letters*, vol. 2, no. 1, pp. 64–71, Jan 2017.
- [3] Y. Onose, Y. Ishida, and Y. Fukuda, "Reproduction of physical function by robot suits," *Proceedings - JSME Conference on Robotics and Mechatronics*, vol. 2, no. 14, 2014.
- [4] J. Klein, S. J. Spencer, and D. J. Reinkensmeyer, "Breaking it down is better: Haptic decomposition of complex movements aids in robot-assisted motor learning," *IEEE Transactions on Neural Systems and Rehabilitation Engineering*, vol. 20, no. 3, pp. 268–275, 2012.
- [5] D. F. P. Granados, B. A. Yamamoto, H. Kamide, J. Kinugawa, and K. Kosuge, "Dance teaching by a robot: Combining cognitive and physical human-robot interaction for supporting the skill learning process," *IEEE Robotics and Automation Letters*, vol. 2, no. 3, pp. 1452–1459, July 2017.
- [6] A. Goswami, M. A. Peshkin, and J. E. Colgate, "Passive robotics: an exploration of mechanical computation," in *Proceedings., IEEE International Conference on Robotics and Automation*, May 1990, pp. 279–284 vol.1.
- [7] K. Koyanagi, J. Furusho, and L.-C. Dong, "Study on force display system using couple of er brakes," in *2004 IEEE/RSJ International Conference on Intelligent Robots and Systems (IROS) (IEEE Cat. No.04CH37566)*, vol. 4, Sept 2004, pp. 3251–3256 vol.4.
- [8] O. Schneider, J. Troccaz, O. Chavanon, and D. Blin, "Padyc: a synergistic robot for cardiac puncturing," in *Proceedings 2000 ICRA. Millennium Conference. IEEE International Conference on Robotics and Automation. Symposia Proceedings (Cat. No.00CH37065)*, vol. 3, 2000, pp. 2883–2888.
- [9] D. K. Swanson and W. J. Book, "Path-following control for dissipative passive haptic displays," in *11th Symposium on Haptic Interfaces for Virtual Environment and Teleoperator Systems, 2003. HAPTICS 2003. Proceedings.*, March 2003, pp. 101–108.
- [10] B. Dellon and Y. Matsuoka, "Path guidance control for a safer large scale dissipative haptic display," in *2008 IEEE International Conference on Robotics and Automation*, May 2008, pp. 2073–2078.
- [11] Y. Hirata, R. Shirai, and K. Kosuge, "Position and orientation control of passive wire-driven motion support system using servo brakes," in *2017 IEEE International Conference on Robotics and Automation (ICRA)*, May 2017, pp. 3702–3707.
- [12] A. A. Stanley and K. J. Kuchenbecker, "Evaluation of Tactile Feedback Methods for Wrist Rotation Guidance," *IEEE Transactions on Haptics*, vol. 5, no. 3, pp. 240–251, 2012.
- [13] J. Van Der Linden, E. Schoonderwaldt, J. Bird, and R. Johnson, "MusicJacket - Combining motion capture and vibrotactile feedback to teach violin bowing," *IEEE Transactions on Instrumentation and Measurement*, vol. 60, no. 1, pp. 104–113, 2011.
- [14] D. Spelmezan, A. Schanowski, and J. Borchers, "Wearable Automatic Feedback Devices for Physical Activities," *Proceedings of the 4th International ICST Conference on Body Area Networks*, p. 1, 2009.
- [15] E. Ruffaldi, A. Filippeschi, A. Frisoli, O. Sandoval, C. A. Avizzano, and M. Bergamasco, "Vibrotactile perception assessment for a rowing training system," *Proceedings - 3rd Joint EuroHaptics Conference and Symposium on Haptic Interfaces for Virtual Environment and Teleoperator Systems, World Haptics 2009*, pp. 350–355, 2009.
- [16] S. Basu, J. Tsai, and A. Majewicz, "Evaluation of Tactile Guidance Cue Mappings for Emergency Percutaneous Needle Insertion," *2016 IEEE Haptics Symposium, HAPTICS 2016*, 2016.
- [17] P. Kapur, S. Premakumar, S. a. Jax, L. J. Buxbaum, A. M. Dawson, and K. J. Kuchenbecker, "Vibrotactile feedback system for intuitive upper-limb rehabilitation," *Proceedings - 3rd Joint EuroHaptics Conference and Symposium on Haptic Interfaces for Virtual Environment and Teleoperator Systems, World Haptics 2009*, pp. 621–622, 2009.
- [18] J. Lieberman and C. Breazeal, "TIKL : Development of a Wearable Vibrotactile Feedback Suit for Improved Human Motor Learning," *IEEE Transactions on Robotics*, vol. 23, no. 5, pp. 919–926, 2007.
- [19] T. McDaniel, M. Goldberg, D. Villanueva, L. N. Viswanathan, and S. Panchanathan, "Motor learning using a kinematic-vibrotactile mapping targeting fundamental movements," *Proceedings of the 19th ACM international conference on Multimedia - MM '11*, p. 543, 2011.
- [20] Y. Jin, H. Chun, G.-H. Yang, and S. Kang, "Vibrotactile cues using tactile illusion for motion guidance," *2013 13th International Conference on Control, Automation and Systems (ICCA S 2013)*, pp. 1064–1067, 2013.
- [21] J. Salazar, Y. Hirata, and K. Kosuge, "Motion Guidance using Haptic Feedback based on Vibrotactile Illusions," *Proceedings of IEEE/RSJ International Conference on Intelligent Robots and Systems (IROS)*, pp. 4685–4691, 2016.
- [22] K. Bark, E. Hyman, F. Tan, E. Cha, S. A. Jax, L. J. Buxbaum, and K. J. Kuchenbecker, "Effects of Vibrotactile Feedback on Human Learning of Arm Motions," *IEEE Transactions on Neural Systems and Rehabilitation Engineering*, vol. 23, no. 1, pp. 51–63, 2015.
- [23] M. Xu, D. Wang, Y. Zhang, and D. Wu, "Effect of vibrotactile cues for guiding simultaneous procedural motion of two joints on upper limbs," in *2015 IEEE/RSJ International Conference on Intelligent Robots and Systems (IROS)*, Sept 2015, pp. 567–572.
- [24] J. V. S. Luces, K. Okabe, Y. Murao, and Y. Hirata, "A phantom-sensation based paradigm for continuous vibrotactile wrist guidance in two-dimensional space," *IEEE Robotics and Automation Letters*, vol. 3, no. 1, pp. 163–170, Jan 2018.
- [25] "Calculating body frame size: Medlineplus medical encyclopedia image." [Online]. Available: <https://medlineplus.gov/ency/imagepages/17182.htm>
- [26] K. Suzuki, T. Thomessen, and M. Niituma, "Phantom Sensation on a Forearm Using a Vibrotactile Interface," *Proceedings of the 2014 JSME Conference on Robotics and Mechatronics*, vol. 14, no. 2, pp. 1–4, 2014, in Japanese.
- [27] S. K. Nagel, C. Carl, T. Kringe, R. Mrtin, and P. Knig, "Beyond sensory substitution: learning the sixth sense," *Journal of Neural Engineering*, vol. 2, no. 4, p. R13, 2005.
- [28] Y. Zheng and J. B. Morrell, "Haptic actuator design parameters that influence affect and attention," in *2012 IEEE Haptics Symposium (HAPTICS)*, March 2012, pp. 463–470.
- [29] C. K. Williams and H. Carnahan, "Motor learning perspectives on haptic training for the upper extremities," *IEEE Transactions on Haptics*, vol. 7, no. 2, pp. 240–250, 2014.
- [30] E. van Breda, S. Verwulgen, W. Saeys, K. Wuyts, T. Peeters, and S. Truijen, "Vibrotactile feedback as a tool to improve motor learning and sports performance: a systematic review," *BMJ Open Sport & Exercise Medicine*, vol. 3, no. 1, 2017.
- [31] O. Khatib, "Real-time obstacle avoidance for manipulators and mobile robots," *The Int. Journal of Robotics Research*, vol. 5, no. 1, pp. 90–98, 1986.
- [32] P. Fitts and M. Posner, *Human Performance*. Brooks/Cole Publishing Company, 1967.